International Journal of Advanced Research in Chemical Science (IJARCS)
Volume 6, Issue 10, 2019, PP 7-21
ISSN No. (Online) 2349-0403
DOI: http://dx.doi.org/10.20431/2349-0403.0610002
www.arcjournals.org

Spectroscopic, Thermal, Fluorescence Studies and Antibacterial Activity of Some Transition Metals with Schiff Base 2-[(2-Furylmethylene) Amino] Benzoic Acid

Omyma Ahmed Moustafa Ali[a]*, Samir Moustafa EL-Medani[b], Abeer Sayed Salama Sayed[b]

[a]*Chemistry Department, Faculty of Women for Arts, Science and Education, Ain Shams University, Cairo, Egypt.*

[b]*Chemistry Department, Faculty of Science, El-Faiyum University, El-Faiyum, Egypt.*

Corresponding Author:** ***Omyma Ahmed Moustafa Ali, *Chemistry Department, Faculty of Women for Arts, Science and Education, Ain Shams University, Cairo, Egypt.*

Abstract: *Complexes of the Schiff base ligand (HL) derived from 2-furancarboxaldehyde and 2-aminobenzoic acid with the metal ions: Cu(II), Ni(II), Co(II), Zn(II), Hg(II), Fe(III), La(III) and Sm(III) have been prepared. The ligand HL and its metal complexes were characterized on the bases of its elemental analyses, IR, ^1H NMR, solid reflectance, magnetic moment, molar conductance and thermal analysis. The complexes were found to have the formulae $[Cu(HL)(AcO)_2].H_2O$, $[M(HL)(AcO)_2H_2O].H_2O$ (M = Ni, Co, Zn and Hg), $[Fe(HL)Cl_3].H_2O$, $[La(HL)(NO_3)_3].2H_2O$ and $[Sm(HL)(ClO_4)_3].2H_2O$. The conductance of complexes was measured and revealed non-electrolyte chelates. Thermal analysis of the complexes were investigated and indicated the presence of hydrated water molecules. The ligand and its complexes were tested by weight loss method and found corrosion inhibition for stainless steel type 410 in 1 M H_2SO_4 medium. Fluorescence and antibacterial activities of the synthesized compoundswere investigated indicating photoactive materials and a considerable biological activity.*

Keywords: *Complexes; Spectral; Fluorescence; Corrosion Inhibition.*

1. INTRODUCTION

Schiff bases are considered as a very important class of organic compounds because of their ability to form stable complexes with many different transition metal ions in various oxidation states [1-10]. These complexes have wide applications in some biological aspects [11-20], catalytic activity [21-22] and fluorescence properties [23]. Several Schiff bases have recently been investigated as corrosion inhibitors for various metals and alloys in acid media [24, 25]. The inhibition of corrosion by Schiff bases can be attributed to its molecules with **π**-electrons of –C=N- groups and **π**-electrons of aromatic ring. Conjugating large p bond through which its molecules are likely to be adsorbed strongly on the metal surface. Coordination numbers of lanthanide complexes are in range from six to twelve, eight and nine being the most common coordination numbers. Lanthanides are weak Lewis acids and preferably coordinate to hard Lewis bases like oxygen. In this paper, we report synthesis of eight Schiff base complexes of Cu(II), Ni(II), Co(II), Zn(II), Hg(II), Fe(III), La(III) and Sm(III)metal ions. The complexes were characterized by elemental analysis, solid reflectance, FT-IR and fluorescence spectroscopy, thermal analysis and molar conductance. Also, the inhibition effects of the studied compounds on the corrosion of stainless steel 410 (SS410) in H_2SO_4 1M solutions were investigated.

Experimental

2. MATERIALS AND METHODS

All chemicals used were of analytical reagent grade (AR) and of the highest purity available. They included 2-furanecarboxaldehyde (Sigma), 2-aminobenzoic acid, $Cu(OAc)_2.H_2O$, $FeCl_3.6H_2O$, $Ni(OAc)_2.4H_2O$, $Co(OAc)_2.4H_2O$, $Zn(OAc)_2.4H_2O$, $Hg(OAc)_2.4H_2O$, $La(NO_3)_3.6H_2O$ and $Sm(ClO_4)_3.6H_2O$ from Aldrich. All solvents were of analytical grade. IR measurements (KBr pellets) were carried out on a Shimadzu 8000 FT-IR spectrometer. ^{1}HNMR spectra were recorded on a BrukerAvance Dry 300 FT-NMR spectrometer in DMSO-d6 with TMS as the internal reference. The mass spectra were recorded on a GCMS-QP 2010 Shimadzu mass spectrometer with DI (direct inlet)

and CI (chemical ionization). Thermo gravimetric analyses (TG and DTG) were carried out under N_2 atmosphere with a heating rate of 10° C/min. using a Shimadzu DT-50 thermal analyzer. Magnetic susceptibility measurements of the paramagnetic complexes in the solid state (Gouy method) were performed on a Sherwood Scientific Magnetic Susceptibility Balance. Microanalyses were performed using JEOL JMS-AX500 elemental analyzer. All conductivity measurements were performed in DMF ($1x10^{-3}$ M) at 25°C, by using Jenway 4010 conductivity meter. UV/Vis diffuse reflectance spectra were measured on a Shimadzu 3101 pc spectrophotometer. The photo luminescent properties of all compounds were studied using a Jenway 6270 Fluorimeter.

2.1. Synthesis of Schiff Base Ligand (HL)

A hot solution of2-aminobenzoic acid(14 mmol) was mixed with a hot solution of 2-furancarboxaldehyde (14 mmol) in 150 ml absolute methanol. The resulting mixture was left under reflux for 4h and the solid product formed was separated by filtration, washed with methanol, and then dried in a vacuum over anhydrous calcium chloride. The yellow powder product is produced in 80% yield.

2.2. Synthesis of Metal Complexes

The metal complexes of the Schiff base, HL, were prepared by the addition of a hot solution of the metal acetate, chloride, nitrate or perchlorate (1 mmol) in an ethanol (25 ml) to the hot solution of the Schiff base (1 mmol) in tetrahydrofurane (THF) solvent (25 ml). The resulting mixture was stirred under reflux for 4 h whereupon the complexes precipitated. They were collected by filtration and washed with diethyl ether.

2.3. Corrosion Test

Gravimetric corrosion measurements (weight loss method) were carried out according to the ASTM standard procedure described in [26]. In brief, stainless steel specimens in triplicate were immersed for a period of 2 h in 100 ml 1 M H_2SO_4 containing various concentrations of the studied inhibitors. The mass of the specimens before and after immersion was determined using an analytical balance accurate to 0.1 mg. Before measurements, the specimens were abraded with a sequence of emery papers of different grades (400, 800, 1000 and 1200), followed by washing with double distilled water and finally degreased with ethanol and dried at room temperature. The composition of the stainless steel type 410 are in wt. % 0.15C, 11Cr, 75Fe, 1Mn, 0.75Ni, 0.04P, 0.03S, 1Si.

2.4. In Vitro Antibacterial Study

The *in vitro* antibacterial activity of the ligand and its complexes were screened against the bacteria *Staphylococcus aureus*, *Bacillus subtilis*, *Escherichia coli* and *Pseudomonas aeruginosa* by the paper disc method using nutrient agar as the medium. The standard disc diffusion method was followed to determine the antibacterial activity of the synthesized compounds. The well (8 mm diameter) was then filled with the test solution and the plates were inoculated at 37°C for 48 h. During this period, the growth of the inoculated microorganisms was affected and then the inhibition zones developed on the plates were measured. The effectiveness of an antibacterial agent was assessed by measuring the zones of inhibition around the well. The diameter of the zone is measured to the nearest millimeter (mm). The antibacterial activity of each compound was compared with that of standard antibiotics such as Tetracycline. DMSO was used as a control under the same conditions for each organism and no activity was found. The activity results were calculated as a mean of triplicates.

3. Results And Discussion

In the present investigation, the Schiff base ligand (HL) and its complexes are synthesize and characterize by different analytical techniques. The isolated solid complexes are stable in air at room temperature, insoluble in water and most organic solvents and soluble in DMF and DMSO solvents. Various attempts to obtain the single crystals of the complexes have so far been unsuccessful. The analytical data along with some physical properties of Schiff base ligand and its complexes are summarized in Table 1.

Table1. Analytical and physical data of the ligand and its complexes

Compound	Color (% yield)	M.Wt.	M.p./ºC	Found(Calculated)			Λ_m (Ω^{-1}mol^{-1}cm^2)
				% C	% H	% N	
$HL(C_{12}H_9NO_3)$	Yellow(80)	215.21	180	66.78(66.97)	4.34(4.21)	6.63(6.51)	–
$CuC_{16}H_{17}NO_8$	Dark brown(70)	414.85	>300	46.65(46.32)	4.04(4.13)	3.42(3.38)	2.5
$NiC_{16}H_{19}NO_9$	Violet(60)	428.04	>300	44.96(44.90)	4.27(4.47)	3.16(3.27)	1.1
$FeC_{12}H_{11}NO_4Cl_3$	Black (80)	395.43	>300	36.10(36.45)	2.47(2.80)	3.65(3.54)	2.9
$CoC_{16}H_{19}NO_9$	Brown(60)	428.26	>300	44.53(44.87)	4.18(4.47)	3.52(3.27)	1.7
$ZnC_{16}H_{19}NO_9$	Dark brown(60)	434.70	>300	44.15(44.21)	4.59 (4.41)	3.69(3.22)	0.01
$HgC_{16}H_{19}NO_9$	Yellow(70)	569.92	>300	33.38(33.72)	3.16 (3.36)	2.17(2.46)	1.1
$LaC_{12}H_{13}N_4O_{14}$	Black(70)	576.16	>300	25.44(25.02)	2.96 (2.27)	9.14(9.72)	3
$SmC_{12}H_{13}NO_{17}Cl_3$	Black(80)	699.94	>300	20.25(20.59)	1.77(1.87)	2.34(2.00)	2.5

3.1. Composition And Structures of HL Schiff Base Complexes

The stoichiometries of the complexes derived from elemental analysis correspond to the general formulae $[Cu(HL)(AcO)_2].H_2O$, $[M(HL)(AcO)_2H_2O].H_2O$ (M = Ni, Co, Zn and Hg), $[Fe(HL)Cl_3].H_2O$, $[La(HL)(NO_3)_3].2H_2O$ and $[Sm(HL)(ClO_4)_3].2H_2O$, Scheme 1. These propositions are also in accord with molar conductivity measurements, TGA, IR, UV-vis and ^{1}H NMR presented in the following sections. The formation of complexes may proceed according to the following equations given below.

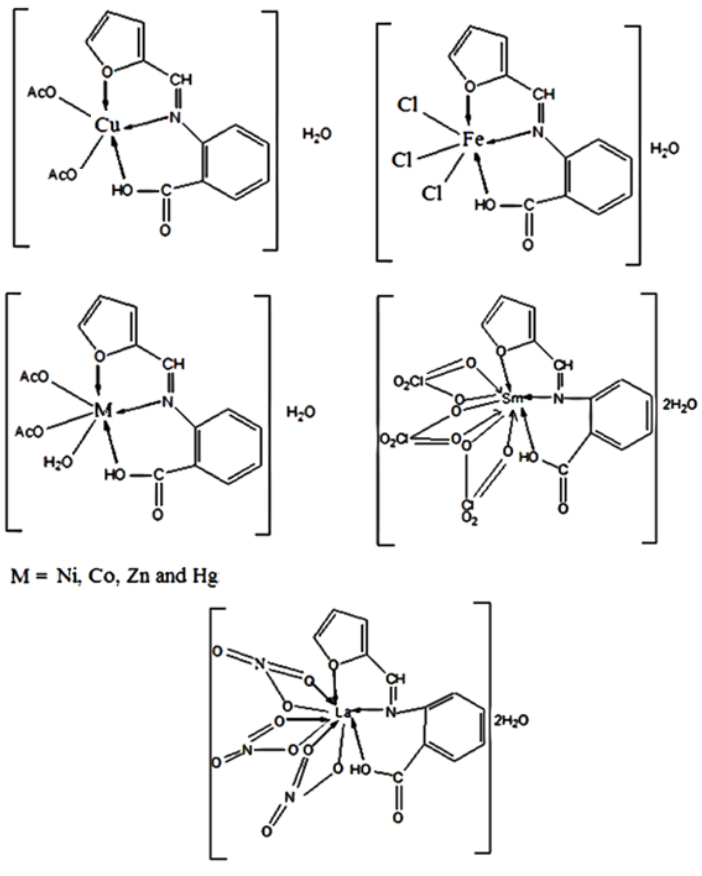

Scheme1. *Structures of complexes*

$Cu(AcO)_2 + HL + H_2O \rightarrow [Cu(HL)(AcO)_2].H_2O$

$M(AcO)_2 + HL + 2H_2O \rightarrow [M(HL)(AcO)_2H_2O].H_2O$

M = Ni (II), Co (II), Zn (II) and Hg (II)

$FeCl_3 + HL + H_2O \rightarrow [Fe (HL) Cl3].H_2O$

$MX_3 + HL + 2H_2O \rightarrow [M (HL) X3].2H_2O$

M=La (III), X= (NO_3) or M=Sm (III), X= (ClO_4)

3.2. Molar Conductivity Measurements

The chelates are dissolved in DMF and the molar conductivities of 10^{-3}M of their solutions at 25 ºC are measured. Table 1 shows the molar conductance values of the complexes. It is concluded from the results that the complexes have a molar conductivity values in the range from 0.1 to 3.0Ω^{-1} mol^{-1} cm^2 indicating non-ionic nature complexes (non-electrolytes).

3.3. IR Spectra and Mode of Bonding

The IR band assignments of the Schiff base ligand and its complexes are given in Table 2. Comparison of the IR spectra of the metal complexes with that of the free ligand revealed that all complexes showed a broad band in the range 3278–3423 cm^{-1} assignable to ν(OH) of the carboxylic acid group, the coordinated and hydrated water molecules. The band at 1666 cm^{-1} assigned to ν(C=N) in the free Schiff base was shifted to lower frequency (1598-1626 cm^{-1}) in all complexes indicating the participation of the azomethine nitrogen in chelation [27]. It is expected that coordination of nitrogen to the metal atom would reduce the electron density in the azomethine link and thus lowering the HC=N bond order. The $\nu_{asym}(COO^-)$ and $\nu_{sym}(COO^-)$ stretching vibrations are observed at 1579 and 1413 cm^{-1} for HL ligand [28]. On complexation, these bands were shifted to 1515–1592 and 1333-1407 cm^{-1}, respectively. A medium intensity band due to ν (C–O–C) stretching vibration of furan appeared at 1255 cm^{-1} in the ligand. This band was shifted to 1223–1288 cm^{-1} in complexes, suggesting coordination through oxygen of furan moiety [23]. Non-ligand IR bands were displayed in the complexes. The triply split band maxima at 1145, 1115, 1087 cm^{-1} and a medium band at 628 cm^{-1} appeared in Sm(III) complex spectrum were attributed to bidentately coordinated perchlorate anion [29, 30]. The IR spectrum of the La(III) complex showed four intense bands at 1456, 1385, 1333 and 818 cm^{-1}. The separation frequency of 123 cm^{-1} between 1456(ν_s) and 1333(ν_{as}) isconsistent with the value reported in literature for the nitrate group coordinated in a bidentate manner [31]. Appearance of new bands in the spectra of complexes in the regions 465–528 cm^{-1} and 422–470 cm^{-1} were assigned to ν(M–O) and ν(M–N) stretching vibration [32].

Table2. *IR data (4000-400 cm^{-1}) of the Schiff base ligand and its complexes*

Compound	IR data(cm^{-1})[a]								
	(OH) or (H2O)	COO^- (asym)	COO^- (sym)	C=N	C–O–C (furan)	M–O (carboxylic)	M–O (furan)	M–N	Other bands
HL	3318(b)	1579(s)	1413(s)	1666(s)	1255(m)	-	-	-	-
$[Cu(HL)(AcO)_2].H_2O$	3278(b)	1558(s)	1384(s)	1604(s)	1288(m)	551(w)	489(w)	451(w)	-
$[Ni(HL)(AcO)_2H_2O].H_2O$	3351(b)	1589(s)	1388(s)	1610(s)	1282(m)	547(w)	476(w)	433(w)	-
$[Fe(HL)Cl_3].H_2O$	3372(b)	1517(s)	1405(s)	1608(s)	1276(m)	563(w)	493(m)	430(w)	-
$[Co(HL)(AcO)_2H_2O].H_2O$	3309(b)	1592(s)	1407(s)	1616(s)	1243(m)	568(w)	472(w)	422(w)	-
$[Zn(HL)(AcO)_2H_2O].H_2O$	3298(b)	1588(s)	1393(s)	1610(s)	1273(m)	525(w)	465(w)	440(w)	-
$[Hg(HL)(AcO)_2H_2O].H_2O$	3423(b)	1583(s)	1359(s)	1607(s)	1267(m)	528(w)	480(w)	428(w)	-
$[La(HL)(NO_3)_3].2H_2O$	3392(b)	1564(sh)	1353(m)	1626(m)	1223(m)	546(w)	484(w)	432(w)	1456, 1385, 1333, 818; (NO_3^-) (bidentate)
$[Sm(HL)(ClO_4)_3].2H_2O$	3367(b)	1515(s)	1333(m)	1598(s)	1254(m)	590(w)	528(w)	470(w)	1145, 1115, 1087, 628; (ClO_4^-) (bidentate)

[a]s, strong; m, medium; w, weak; b, broad.

3.4. ^{1}H NMR Spectra

There is good agreement between the ^{1}H NMR spectra of the prepared compounds and their assigned structures. The chemical shifts of the different types of protons in the ^{1}H NMR spectra of the HL ligand and its diamagnetic Zn(II), Hg(II) and La(III) complexes are listed in Table 3. The ^{1}H NMR spectrum of the ligand HL (Fig. 1) exhibited a broad signal at 12.69 ppm due to hydrogen-bonded carboxylic proton [33]. This signal appeared in the ^{1}H NMR spectra of complexes at 9.62-10.20 ppm with up-field shifts, indicating the coordination of carboxylic oxygen to metal without proton displacement. The ligand also showed a singlet at 8.32 ppm for -CH=N which was shifted to 8.21-8.31 ppm in the complexes indicating the involvement of azomethine group in complexation [34]. In addition, the peaks due to hydrogen of the aromatic and furan species are slightly shifted to up ordown-field supporting the coordination of the ligand HL to metal ions.

Table3. *Theimportant ^{1}H NMR data for ligand, HL and its complexes*

Compound	Chemical shift, δ (ppm)	Assignment
HL	12.69 8.32 6.47–7.8	(s, 1H, COOH) (s,1H, azomethine) (m, 7H, 4ArH and 3 furan H)
$[Zn(HL)(AcO)_2H_2O]H_2O$	10.20 8.21 6.42–7.87 3.33 1.83	(s, 1H, COOH) (s,1H, azomethine) (m, 7H, 4ArH and 3 furan H) (s, 4H, H_2O) (s, 6H, CH_3COO)
$[Hg(HL)(AcO)_2H_2O]H_2O$	9.80 8.31 6.43–7.95 3.15 1.90	(s, 1H, COOH) (s,1H, azomethine) (m, 7H, 4ArH and 3 furan H) (s, 4H, H_2O) (s, 6H, CH_3COO)
$[La(HL)(NO_3)_3]$ $2H_2O$	9.62 6.46-8.43 3.34	(s, 1H, COOH) (m, 8H, azomethine H, 4ArH and 3 furan H) (s, 4H, H_2O)

s, singlet; d, doublet; m, multiplet; b, broad

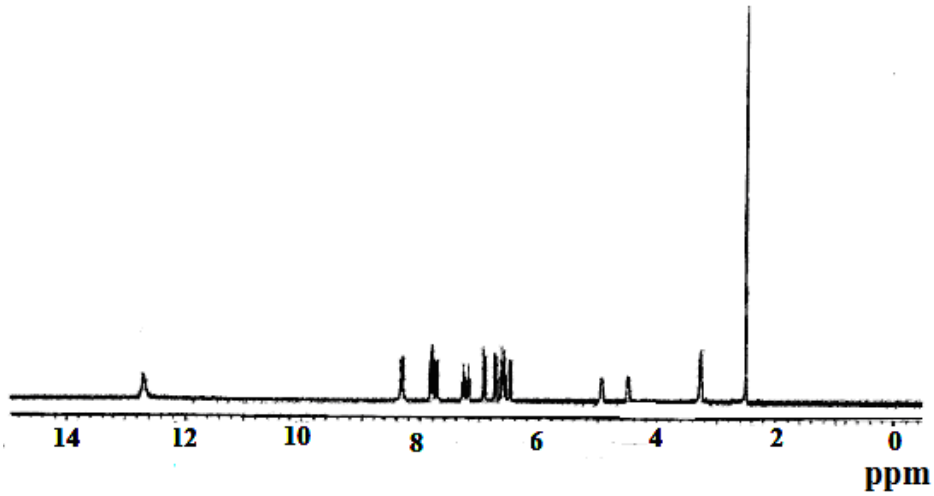

Fig1. *^{1}H NMR spectrum of HLligand.*

3.5. Mass Spectra

The mass spectrum of the ligand (Fig. 2) showed the molecular ion peak at 215, confirming its formula weight (F.W. 215.21). The mass spectra of the Cu(II), Ni(II), Co(II), Zn(II), Hg(II) and Fe(III) complexes provide good evidence for the molecular formulas of these complexes (S1-S6). The most prominent mass spectral peaks of the reported complexes are given in Table 4.They can be discussed as follows:

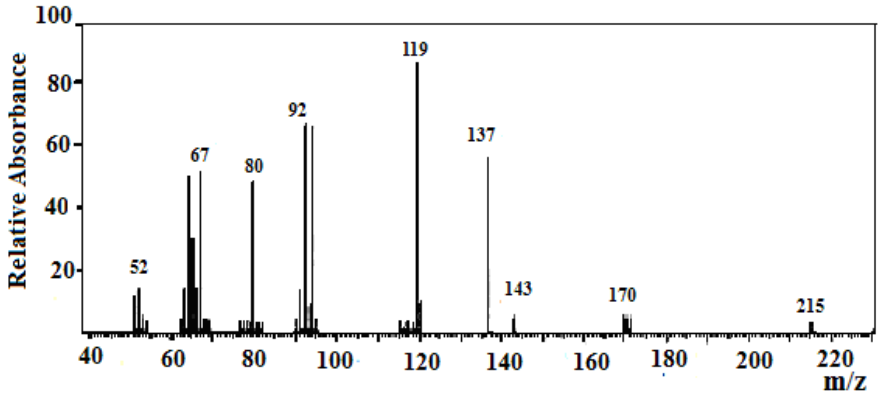

Fig2. *Mass spectrum of the ligand HL.*

Table4. *The diffuse reflectance data of the Schiff base (HL) and its complexes*

Compound	λ_{max} (nm)	Band assignment
HL	269 340 514	π→π* n→π* charge transfer
$[Cu(HL)(AcO)_2].H_2O$	264 313 347 410, 612	π→π* n→π* charge transfer d-d transitions
$Ni(HL)(AcO)_2H_2O].H_2O$	285 315 358 456, 660, 700	π→π* n→π* charge transfer d-d transitions
$[Fe(HL)Cl_3].H_2O$	259 326 350 470, 614, 655	π→π* n→π* charge transfer d-d transitions
$[Co(HL)(AcO)_2H_2O].H_2O$	242 268 332 424, 571, 606	π→π* n→π* charge transfer d-d transitions
$[Zn(HL)(AcO)_2H_2O].H_2O$	257 354 411, 465	π→π* n→π* charge transfer
$[Hg(HL)(AcO)_2H_2O].H_2O$	260 326 460	π→π* n→π* charge transfer
$[La(HL)(NO_3)_3].2H_2O$	268 304, 335 407	π→π* n→π* charge transfer
$[Sm(HL)(ClO_4)_3].2H_2O$	239 344, 376 418, 470 539, 570, 606	π→π* n→π* charge transfer f-f transitions

$[Cu(HL)(AcO)_2].H_2O$: The molecular ion peak is observed at 414 (67.27 %) (Calc.414.85). The presence of a peak at 216 (69.09 %) indicated the presence of ligand in the complex. The removal of the coordinated water molecule was indicated by the peak at 397 (47.27 %) (Calc.396.83). This fragment ion underwent fragmentation with a loss of 2-acetate groups to give a peak at 277 (83.64 %). Further fragmentation with the loss of the HL ligand gave a peak at 64 (71.82 %).

$Ni(HL)(AcO)_2H_2O].H_2O$: The molecular complex ion peak is showed at 428 (44.52 %). The existence of the ligand was indicated by the peak at 214. The removal of hydrated and coordinated water molecules are indicated by two peaks at 410 (52.05 %) and 390 (48.63 %), respectively. This

fragment ion underwent fragmentation with the loss of the 2-acetate groups giving a peak at 274 (67.12 %) (Calc. 273.93). Further fragmentation gave a peak at 61 due to loss of the ligand (HL).

$[Fe(HL)(Cl)_3].H_2O$: The molecular ion peak of the complex isobserved at 395 (91.30 %) (Calc. 395.43). The removal of ligand (HL) was indicated by the ion peak at 179 (63.04 %) (Calc. 180.36). The removal of one chlorine atom and a hydrated water molecule are indicated by the peaks at 147 and 128, respectively.

$[Co(HL)(AcO)_2H_2O].H_2O$: The molecular ion peak of the complex isobserved at 428 (91.49 %). The removal of two acetate groups gave a peak at 310 (75.53 %) (Calc. 310.17). This fragment ion underwent fragmentation with the loss of a hydrated water molecule giving a peak at 292 (60.64 %). Further fragmentation ion peak was observed at 59 (78.72 %) (Calc. 58.93) referred to the loss of both a ligand molecule and H_2O.

$[Zn(HL)(AcO)_2H_2O].H_2O$: The molecular ion peak is observed at 434 (100.00 %) (Calc. 434. 70). The existence of ligand (HL) is indicated by the peak at 213 (92.11 %) (Calc. 215.21). The removal of the coordinated water molecule is indicated by the peak at 415 (64.04 %) (Calc. 416.68). This fragment ion underwent fragmentation with loss of water molecule and 2-acetate groups gave two peaks at 398 and 280 (52.63 and 54.39 %) (Calc. 398.66 and 280.58), respectively. Further fragmentation with the loss of the HL ligand gave a peak at 63 (52.63 %) (Calc. 65.37 amu).

$[Hg(HL)(AcO)_2H_2O].H_2O$: The molecular ion peak is shown at 569 (80.91 %) (Calc. 569.92). The existence of ligand is indicated by the peak at 214 (60.01 %). The removal of hydrated and coordinated water molecules are indicated by two peaks at 550 (51.82 %) and 534 (73.64 %), respectively. This fragment ion underwent fragmentation with the loss of the 2-acetate groups gave a peak at 476 (73.64 %) and 414 (57.29 %) (Calc. 474.85 and 415.80). Further fragmentation with loss of the ligand (HL) gave a peak at 202 (57.27 %) (Calc. 200.59).

3.6. Magnetic Moments and Electronic Spectra

In this part, we would like to elucidate the important role played by magnetic and electronic spectra in determining the geometrical structures of the investigated metal complexes. The diffuse reflectance spectra of the Schiff base ligand exhibited three bands at 269, 340 and 514 nm which may be assigned to π-π*, n-π* and charge transfer transition. The data are summarized in Table 4.

A square-pyramidal structure is proposed for Cu(II) complex based on the presence of two bands at 612 and 410 nm[35]**.** These may be assigned to $^2B_{1g}\rightarrow{}^2A_{1g}$ and $^2B_{1g}\rightarrow{}^2E_g$ transitions, respectively. The value of the magnetic moment (1.79 B.M.) is in accordance with previous results. The Ni(II) complex has magnetic moment value of 3.81 B.M., which is in the normal range of octahedral Ni(II) complex (μ_{eff} = 2.82 B.M.). The electronic spectrum of Ni (II) complex displayed three bands in the solid reflectance spectrum at v_1 (700 nm: $^3A_{2g}\rightarrow{}^3T_{2g}$); v_2 (660 nm: $^3A_{2g}\rightarrow{}^3T_{1g}(F)$) and v_3 (456 nm: $^3A_{2g}\rightarrow{}^3T_{1g}(P)$) [36]. The spectrum showed also a band at 358 nm which may attribute to ligand to metal charge transfer. The diffuse reflectance spectrum of Fe(III) complex exhibits a band at 470 nm which may be assigned to $^6A_{1g}\rightarrow T_{2g}(G)$ transition in octahedral geometry of the complex [37]. The $^6A_{1g}\rightarrow{}^5T_{1g}$ transition appears to be split into two bands at 614 and 655 nm. The observed magnetic moment of Fe (III) complex is 5.73 B.M. indicating octahedral geometry [38]. The spectrum shows also a band at 350 nm which may attributed to ligand to metal charge transfer. The diffuse reflectance spectrum of the Co (II) complex showed three bands at 424, 571 and 606 nm. The bands observed are assigned to the transition $^4T_{1g}$ (F) $\rightarrow$ $^4T_{1g}$ (P) (v_3), $^4T_{1g}$ (F) $\rightarrow{}^4A_{2g}$ (F) (v_2) and $^4T_{1g}$ (F) $\rightarrow{}^2T_{2g}$ (F) (v_1), respectively, suggesting octahedral structure around Co(II) ion [38]. The magnetic moment value of Co (II) complex has been found to be 4.52 BM corresponding to three unpaired electrons within the range of high spin octahedral complex of Co(II) ion [34]. The diffuse reflectance spectra of Zn(II), Hg(II), La(III) and Sm(III) complexes, showed π–π* and n–π* bands in addition to another bands displayed in the range 407 to 470 nm attributed to ligand to metal charge transfer. The shift of these bands in the spectra of complexes indicated the formation of their metal complexes. As expected for the diamagnetic Zn(II) and Hg(II) (d^{10}) and La(III) (d^0) configurations, ligand field band due to *d-d* electronic transitions is not expected [39] and the trends observed for the ligand were maintained after coordination.

3.7. Luminescence spectral study

The fluorescence characteristic of the ligand HL and its complexes were listed in Table 5. The free ligand exhibits a broad emission band at 405 nm in DMSO solution when excited at 348 nm due to intraligand π→π* transitions. All complexes (Fig. 3) exhibited a blue shift. The spectra of metal complexes exhibited a strong fluorescence emission band in the range 397-462 nm. Co(II) complex upon excitation at 320 nm gives a broad emission band at 462 nm with fluorescence intensity 3887 and a shoulder at 399 nm. The intensity of emission of this band is decreased with respect to ligand. Significant differences in the positions of emission maximum of Schiff base and its complexes establish the coordination of the metal ion to the ligand. The Zn (II) and Fe (III) complexes gave a highly fluorescence properties than other complexes and free ligand. Thus, this study introduce new compounds could be anticipated as potential fluorescence materials in visible light [40].

Table5. *Fluorescence data of HL ligand and its complexes*

Compound	λ_{ex} (nm)	λ_{em}(nm)
HL	348	405
$[Cu(HL)(AcO)_2].H_2O$	348	405
$[Ni(HL)(AcO)_2H_2O].H_2O$	306	399
$[Fe(HL)Cl_3].H_2O$	334	397
$[Co(HL)(AcO)_2H_2O].H_2O$	320	399, 462
$[Zn(L)(AcO)_2H_2O].H_2O$	338	398
$[Hg(L)(AcO)_2H_2O].H_2O$	338	398
$[La(HL)(NO_3)_3].2H_2O$	328	397
$[Sm(HL)(ClO_4)_3].2H_2O$	356	402

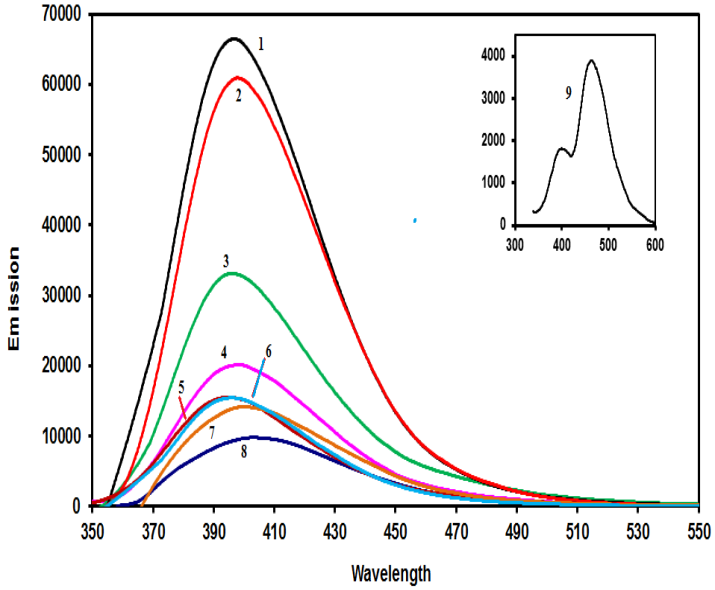

Fig3. *Emission spectra of: (1) $[Zn(HL)(AcO)_2H_2O]H_2O$; (2) $[Fe(HL)Cl_3]H_2O$ (3) $[Ni(HL)(AcO)_2H_2O]H_2O$; (4) $[Cu(HL)(AcO)_2H_2O]$; (5) $[La(HL)(NO_3)_3]2H_2O$; (6) $[Hg(HL)(AcO)_2H_2O]H_2O$; (7) $[Sm(HL)(ClO_4)_3]2H_2O$; (8) Schiff base ligand HL and (9) $[Co(HL)(AcO)_2H_2O]H_2O$.*

3.8. Thermal Analysis

The presence of water molecules and the thermal decomposition studies of the complexes could be achieved by thermal analysis. The TGA results of the Schiff base and its complexes are listed in Table 6.

Table6. *Thermogravimetric data of ligand and its complexes*

Compound	TG range (°C)	Mass loss	Assignment	Metallic residue(%)
		% Found (Calc.)		Found (Calc.)
HL	26–387	44.33 (44.19)	Loss of C_5H_5NO	-
	387–752	55.67 (55.81)	Loss of $C_7H_4O_2$	
$[Cu(HL)(AcO)_2].H_2O$	50–186	4.14 (4.34)	Loss of H_2O	CuO 19.19 (19.18)
	186–955	76.67 (76.48)	Loss of 2(AcO) and HL	

$[Ni(HL)(AcO)_2H_2O].H_2O$	29–76 76–629	4.22 (4.21) 77.89 (78.34)	Loss of H_2O Loss of H_2O, 2(AcO) and HL	NiO 17.89 (17.45)
$[Fe(HL)Cl_3].H_2O$	39–140 140–1000	4.46 (4.55) 75.35 (75.26)	Loss of H_2O Loss of 3Cl and HL	$1/2Fe_2O_3$ 20.19 (20.19)
$[Co(HL)(AcO)_2H_2O].H_2O$	40–100 100–610	4.71(4.21) 82.11 (82.03)	Loss of H_2O Loss of H_2O, 2(AcO) and HL	CoO 13.18 (13.76)
$[Zn(L)(AcO)_2H_2O].H_2O$	34–133 133–573	4.15 (4.14) 77.67 (77.14)	Loss of H_2O Loss of H_2O, 2(AcO) and HL	ZnO 18.18 (18.72)
$[Hg(L)(AcO)_2H_2O].H_2O$	29–98 98–265 265-849	3.15 (3.16) 61.49 (61.64) 35.36 (35.20)	Loss of H_2O Loss of H_2O, 2(AcO) and HL Loss of Hg	No residue
$[La(HL)(NO_3)_3].2H_2O$	38–125 125–414 414–999	6.32 (6.25) 32.31 (32.29) 33.00 (33.19)	Loss of $2(H_2O)$ Loss of $3(NO_3)$ Loss of HL	$1/2La_2O_3$ 28.37 (28.27)
$[Sm(HL)(ClO_4)_3].2H_2O$	30–208 208–492 492–730	5.18 (5.15) 42.35 (42.62) 27.58 (27.32)	Loss of $2(H_2O)$ Loss of $3(ClO_4)$ Loss of HL	$1/2Sm_2O_3$ 24.89(24.91)

The TGA curve of Schiff base HL exhibits a first mass loss of 44.33 % (Calc. 44.19 %) at 26–387 ºC attributed to the liberation of C_5H_5NO moiety. In the 2nd stage within the temperature range 387–752 ºC, the ligandloses the remaining part with mass loss of 55.67 % (Calc. 55.81 %). This decomposition step assigned to the elimination of $C_7H_4O_2$ organic moiety.

The TGA curve of the Cu (II) complex showed two decomposition steps within the temperature range 50–955 ºC. The first step corresponds to the loss of a hydrated water molecule, with a mass loss of 4.14 % (Calc. 4.34 %). The second step of decomposition within the temperature range 186–955 ºC with a net weight loss of 76.67 % (Calc. 76.48 %). This decomposition step has been assigned to the elimination of $2(AcO^-)$ and ligand species to give finally CuO as a residue.

The TGA curve of the Ni(II) complex (Fig. 4) showed two stages of decomposition within the temperature range 29–629 ºC. The first stage at 29–76 ºC corresponded to the loss of water molecule of hydration. The second stage involves the loss of a coordinated water molecule, two acetate groups and a ligand molecule to give finally NiOas a residue.

The TGA curve of Fe(III) complex(Fig. 4)exhibited two decomposition steps within the temperature range 39–1000 ºC. The first decomposition step is within the temperature range 39–140 ºC corresponding to the loss of a hydrated water molecule. The second step was corresponded to the removal of $3Cl^-$ + HL with a net weight loss of 75.35 % (Calc. 75.26 %) leaving $1/2Fe_2O_3$ as a residue.

The TG curve of Co(II) complex displayed a similar decomposition pattern with two decomposition steps. The first decomposition step is consistent with the loss of a hydrated water molecule, whereas the second step involved removal of a coordinated water molecule, two acetate groups and organic ligand moiety, leaving CoOas a residue.

The TGA curve of the Zn (II) complex showed two decomposition steps within the temperature range 34–573 ºC. The first step of decomposition corresponds to the loss of a hydrated water molecule, with a mass loss of 4.15 % (Calc. 4.14 %). The second decomposition step has been assigned to the elimination of a coordinated H_2O, $2(AcO^-)$ and a ligand moiety to give finally ZnOas a residue.

The TGA curve of the Hg(II) complex (Fig. 4) showed three decomposition stages within the temperature range 29–849 ºC. The first stage at 29–98 ºC corresponds to the loss of a hydrated water molecule, with a mass loss of 3.15 % (Calc. 3.16 %). The second stage involves a loss of coordinated water molecule, two acetate moieties and ligand molecule. The third stepwascorresponded to the loss of Hgwithout any residue due to the evaporation of Hg.

The TGA curve of La(III) complex exhibited three decomposition steps within the temperature range 38–999 ºC. The first decomposition step was corresponded to the loss of two hydrated water molecules, with a mass loss of 6.32 % (Calc. 6.25 %). The second and third steps correspond to the removal of $3(NO_3^-)$ and a ligand molecule, respectively leaving $1/2La_2O_3$ as a residue.

The TG curve of $[Sm(HL)(ClO_4)_3].2H_2O$ complex (Fig. 4) displayed a similar decomposition pattern with three decomposition steps. The first decomposition step is consistent with loss of two hydrated water molecules, whereas the second and third steps involved removal of $3(ClO_4^-)$ species and an organic ligand moiety, respectively leaving $1/2Sm_2O_3$ as a final residue.

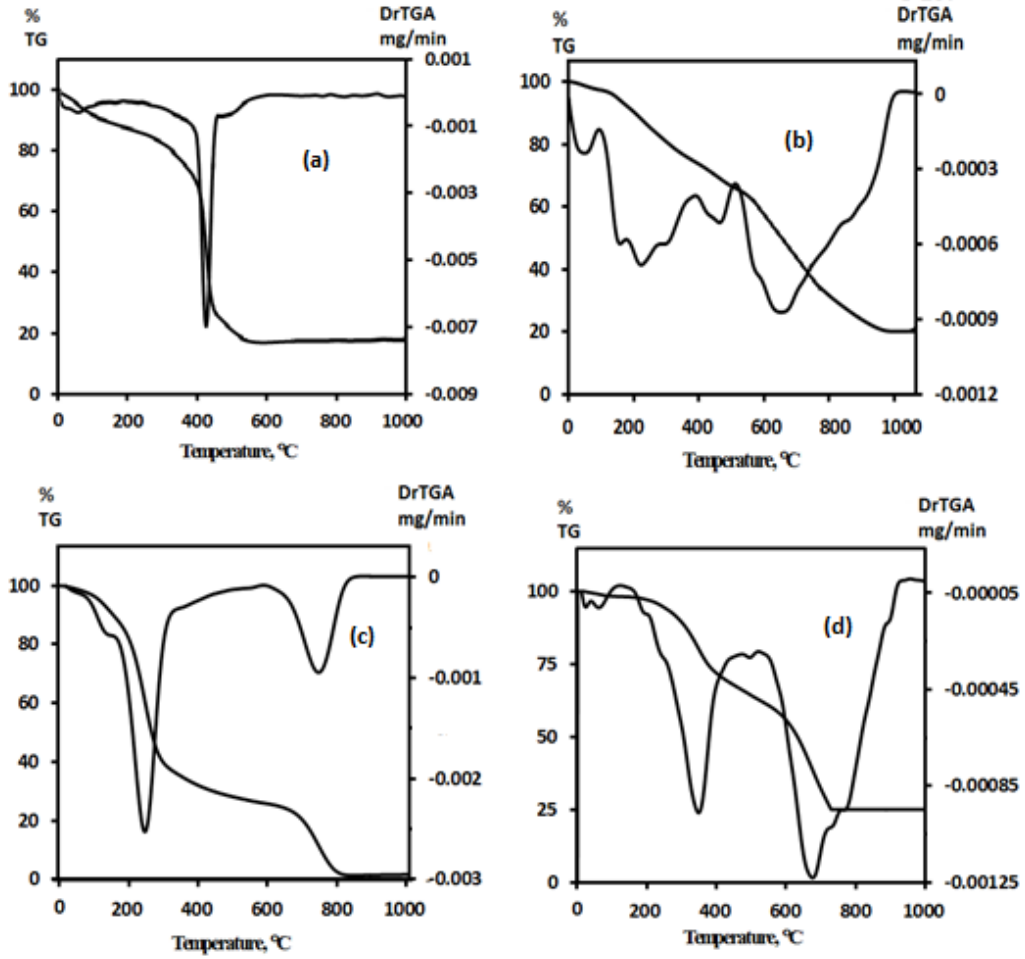

Fig4. *TG and DTG curves of : (a) [Ni(HL)(AcO)$_2$H$_2$O]H$_2$O; (b) [Fe(HL)Cl$_3$]H$_2$O; (C) [Hg(HL)(AcO)$_2$H$_2$O]H$_2$O and (d) [Sm(HL)(ClO$_4$)$_3$]2H$_2$O*

3.9. Corrosion Inhibition

Weight loss measurements of the SS in 1M H_2SO_4 in the absence and the presence of different concentrations of the studied inhibitors were carried out at 25 ºC and the results are reported in Table 7. As shown from the results, the corrosion rate (R) of the SS decreased in the presence of the additives and the inhibition efficiency increased with the increase in the inhibitor concentration (Fig. 5) [23].The maximum efficiency of the ligand on stainless steel 410, is 78 % at 1 x 10^{-3} M HL concentration,. The maximum efficiencies for the Cu(II), Ni(II) and Co(II) complexes are 74 % for 1 x 10^{-4} M $[Cu(HL)(AcO)_2].H_2O$, 92 % for 1 x 10^{-3} M $[Ni(HL)(AcO)_2H_2O].H_2O$ and 62 % for 1 x 10^{-4} M $[Co(HL)(AcO)_2H_2O].H_2O$. Also, the maximum efficiencies for Zn(II), Hg(II) and La(III) complexes are 88 % for the concentration of 1 x 10^{-3} M $[Zn(HL)(AcO)_2H_2O].H_2O$, 80 % for the concentration of 1 x 10^{-5} M $[Hg(HL)(AcO)_2H_2O].H_2O$ and 89 % for the concentration of 1 x 10^{-3} M $[La(HL)(NO_3)_3].2H_2O$. A concentration of 10^{-4} M of La (III) and Zn (II) complexes gives the highest value for inhibition efficiency. This indicates a good corrosion inhibition for stainless steel 410. The inhibition efficiency of these compounds can be illustrated on the basis of their larger molecular size and electron donating nature leading to a larger surface coverage of the metal and high bond strength between the molecule and the metal surface. This was indicated by the fact that: with increasing the inhibitor concentration, both (θ) and (η) were increased while (R) was reduced (Table 7). So, the dissolution of stainless steel in the presence of the investigated inhibitors can be interpreted on the basis of interface inhibition mode, the inhibitors act effectively at the metal solution interface [41].

Table7. *Corrosion parameters of stainless steel 410 in 1M H_2SO_4 at different concentrations of inhibitors.*

Inhibitor	C_{inh}(M)	R(mg cm^{-2} h^{-1})	θ	η (%)
Blank	-	0.88	-	-
HL	$1x10^{-4}$	0.58	0.40	40
	$5x10^{-4}$	0.35	0.60	60
	$1x\ 10^{-3}$	0.20	0.78	78
$[Cu(HL)(AcO)_2].H_2O$	$1x\ 10^{-5}$	0.48	0.50	50
	$5x10^{-5}$	0.26	0.71	71
	$1x\ 10^{-4}$	0.23	0.74	74
$[Ni(HL)(AcO)_2H_2O].H_2O$	$1x\ 10^{-4}$	0.20	0.74	74
	$5x10^{-4}$	0.11	0.88	88
	$1x\ 10^{-3}$	0.07	0.92	92
$[Co(HL)(AcO)_2H_2O].H_2O$	$1x\ 10^{-6}$	0.30	0.30	30
	$1x\ 10^{-5}$	0.47	0.46	46
	$1x\ 10^{-4}$	0.34	0.62	62
$[Zn(HL)(AcO)_2H_2O].H_2O$	$1x10^{-5}$	0.33	0.62	62
	$1x10^{-4}$	0.17	0.81	81
	$1x10^{-3}$	0.10	0.88	88
$[Hg(HL)(AcO)_2H_2O].H_2O$	$1x10^{-6}$	0.58	0.34	34
	5×10^{-6}	0.40	0.55	55
	$1x10^{-5}$	0.18	0.80	80
$[La(HL)(NO_3)_3].2H_2O$	$1x10^{-5}$	0.40	0.55	55
	$1x10^{-4}$	0.17	0.81	81
	$1x10^{-3}$	0.10	0.89	89

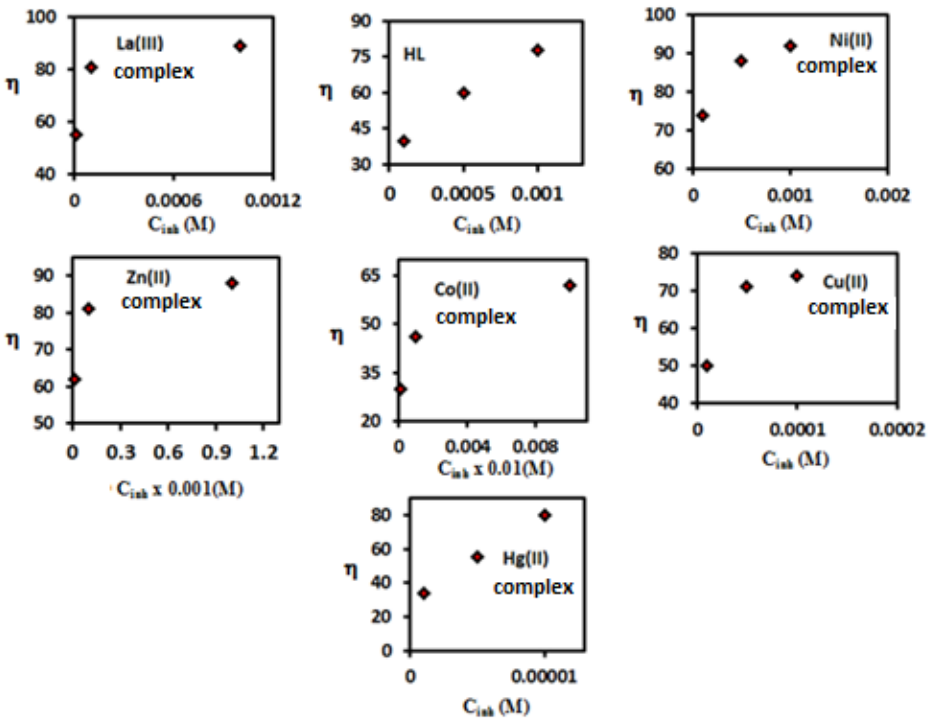

Fig5. *Plot of inhibition efficiency against inhibitor concentrations.*

3.10. Antibacterial Activity

The Schiff base HL ligand and its metal complexes are evaluated for antibacterial activity against two Gram-positive bacteria (*B. Subtilis* and *S. aureus*) and two Gram-negative bacteria (*E.coli* and *P. aeruginosa*). The antibacterial activities of the prepared compounds are listed in Table 8. All the investigated compounds showed a remarkable biological activity against bacteria (Fig. 6).The obtained results reflect that; (1) The metal complexes of Cu(II), Ni(II) and La(III) possess moderate antibacterial activity; (2) Fe(III) and Sm(III) complexes showed low activity against all studied

bacteria; (3) Co (II) and Zn (II) complex showed higher antibacterial activity more than that of ligand; (4) Hg(II) complex against *S. aureus* is more potent than the standard antibiotics and showed the highest activity against *B. Subtilis* and *E. Coli*. (5) Hg(II) complex against *P. aeruginosa* is the same activity as the standard antibiotics. On chelation, the delocalization of π-electrons over the whole chelate ring will be increased which enhances the penetration of the complexes into lipid membranes and blocking the metal binding sites in the enzymes of microorganisms. Also, the tested complexes may disturb the respiration process of the cell and consequently block the synthesis of proteins leading to no further growth of the organisms [42]. The variation in the activity values of different compounds against different organisms depends on either the impermeability of the cells of the microbes or on the differences in ribosome of microbial cells.

Table8. *Antibacterial activities of ligand and its complexes*

Compound	Diameter of inhibition zone (mm)			
	Bacillus Subtilis (G^+)	Staphylococcus Aureus (G^+)	Escherichia Coli (G^-)	Pseudomonas Aeruginosa (G^-)
HL	13	12	11	14
$[Cu(HL)(AcO)_2].H_2O$	10	13	11	13
$[Ni(HL)(AcO)_2H_2O].H_2O$	13	15	13	13
$[Fe(HL)Cl_3].H_2O$	9	13	10	10
$[Co(HL)(AcO)_2H_2O].H_2O$	16	14	14	16
$[Zn(HL)(AcO)_2H_2O].H_2O$	16	15	17	17
$[Hg(HL)(AcO)_2H_2O].H_2O$	27	31	28	29
$[La(HL)(NO_3)_3].2H_2O$	12	12	13	10
$[Sm(HL)(ClO_4)_3].2H_2O$	9	9	9	9
Standard:Tetracycline Antibacterial agent	31	28	30	29

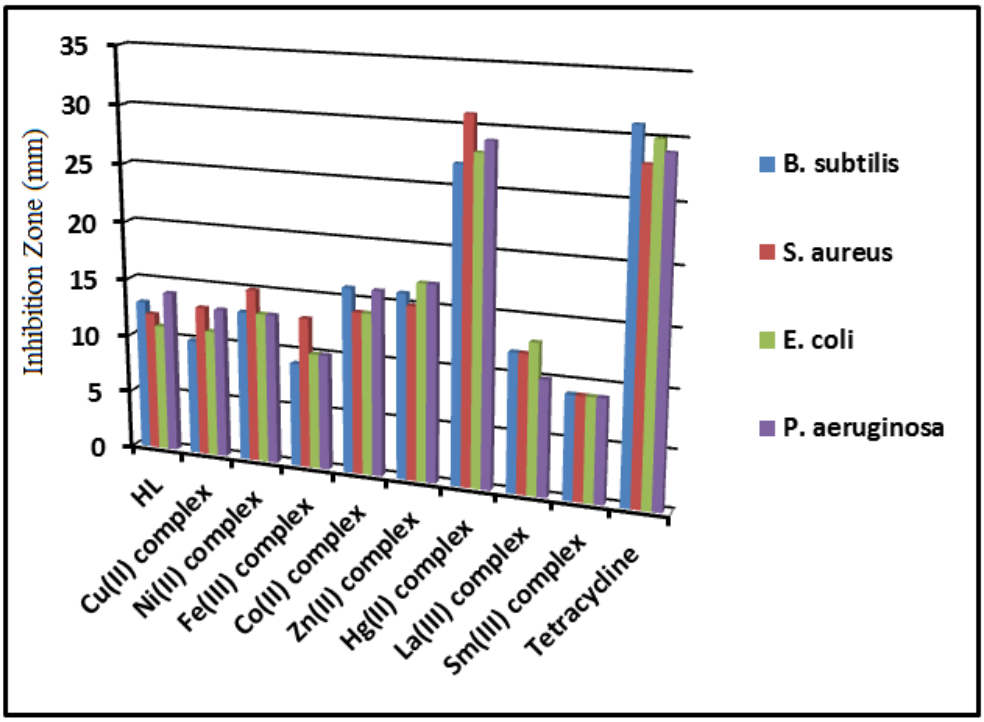

Fig6. *Antibactirial activity of compounds under study*

4. CONCLUSION

A series of eight mononuclear complexes are synthesize and characterize by elemental analysis, TGA, spectral analysis like ^1H NMR, Solid Reflectance, FT-IR and Mass Spectrometry. The results support the suggested structure of metal complexes. Conductance measurements showeda non-electrolyte nature of complexes. The studies suggest the coordination of the Schiff base (HL) to metals is in its protonated form acting as tridentate NON ligand. Thermal studies indicated high stability complexes. Fluorescence studies showed that the reported ligand and its complexes can potentially serve as

photoactive materials. The corrosion inhibition data showed that HL and its complexes are efficient corrosion inhibitors for stainless steel type 410. Furthermore, the novel complexes exhibit considerable antibacterial activity against *B. subtilis, S. aureus, E. coli* and *P. aeruginosa,* in comparison with the standard drug *tetracycillin*.

REFERENCES

[1] Taha ZA, AjlouniAM, Al-Hassan KA, Hijazi AK, Faiq AB.(2011). Syntheses, characterization, biological activity and fluorescence properties of bis-(salicylaldehyde)-1, 3-propylenediimine Schiff base ligand and its lanthanide complexes. SpectrochimActa, Part A.81:317–23.

[2] Abd El-Halim HF, Nour El-Dien FA, Mohamed GG, Mohamed NA. (2013). Chelating behavior, thermal studies and biocidal efficiency of tioconazole and its complexes with some transition metal ions.J ThermAnal Calorim.111:173–81.

[3] Manav N, Gandhi N, Kaushik NK. (2000). Some tribenzyltin(IV) complexes with thiohydrazides and thiodiamines. synthesis, characterization and thermal studies. J Therm Anal Calorim.61:127–34.

[4] Chaudhary A, Bansal N, Gajraj A, Singh RV. (2003). Antifertility, antibacterial, antifungal and percent disease incidence aspects of macrocyclic complexes of manganese(II). J InorgBiochem.96:393-400.

[5] Soliman MH, Mohamed GG, Mohamed EA. (2010). Metal complexes of fenoterol drug.J Therm Anal Calorim.99:639–47.

[6] Radecka-Paryzek W, Patroniak V, Lisowski J. (2005). Metal complexes of polyaza and polyoxaaza Schiff base macrocycles. CoordChem Rev, 249:2156–75.

[7] Rezaeivalaa M, Keypour H. (2014). Schiff base and non-Schiff base macrocyclic ligands and complexes incorporating the pyridine moiety—the first 50 years. CoordChem Rev.280:203–53.

[8] Andruh M. (2015). The exceptionally rich coordination chemistry generated by Schiff-base ligands derived from o-vanillin. Dalton Trans. 44:16633–53.

[9] Gupta AK, Pal R. (2015). Dehydroacetic acid based Schiff bases and their metal complexes: a review. World J Pharm Pharmacol Sci. 4:386-425.

[10] Sadeek SA, Refat MS. (2006). Preparation and characterization of Tin(II) complexes with isomeric series of Schiff bases as ligands. J Korean Chem Soc.50:107–15.

[11] Bukonjic´ AM, Tomovic´ DLJ, Nikolic´ MV, Mijajlovic´ MZ, Jevtic´ VV, Ratkovic´ ZR, Novakovic´ SB, Bogdanovic´ GA, Radojevic´ ID, Maksimovic´ JZ, Vasic´ SM, C ˇ omic´ LR, Trifunovic´ SR, Radic´ GP. (2017). Antibacterial, antibiofilm and antioxidant screening of copper (II) complexes with some S-alkyl derivatives of thiosalicylic acid. Crystal structure of the binuclear copper(II)-complex withS-propyl derivative of thiosalicylic acid. J MolStruct.1128:330-7.

[12] Gandra RM, Mc Carron P, Fernandes MF, Ramos LS, Mello TP,Aor AC, Branquinha MH, McCann M, Devereux M, Santos ALS .(2017). Antifungal potential of Copper (II), Manganese (II) and Silver (I) 1, 10-phenanthroline chelates against multidrug-resistant fungal species forming the Candida haemulonii complex: impact on the planktonic and biofilm lifestyles. Front Microbiol. 8:1-11.

[13] Olar R, Vlaicu ID, Chifiriuc MC, Bleotu C, Stanica˘ N, VasileSca˘et¸eanu G, Silvestro L, Dulea C, Badea M. (2017). Synthesis, thermal analysis and biological characterisation of some new nickel (II) complexes with unsaturated carboxylates and heterocyclic N-donor ligands.J Therm Anal Calorim.127:731–41.

[14] Zayed EM, Mohamed GG, Hindy AMM. (2015). Transition metal complexes of novel Schiff bases synthesis, spectroscopic characterization, and in vitro antimicrobial activity of complexes.J Therm Anal Calorim.120:893–903.

[15] Kalinowska M, Swiderski G, Matejczyk M, Lewandowski W. (2016). Spectroscopic,thermogravimetric and biological studies of Na(I),Ni(II) and Zn(II) complexes of quercetin. JThermAnalCalorim.126:141–8.

[16] Dhahagani K, Kumar SM, Chakkaravarthi G, Anitha K, Rajesh J,Ramu A, Rajagopal G. (2014). Synthesis and spectral characterization of Schiff base complexes of Cu(II), Co(II), Zn(II) and VO(IV) containing 4-(4-aminophenyl) morpholine derivatives: antimicrobial evaluation and anticancer studies. SpectrochimActa, Part A. 87:94-117.

[17] Prabhakaran R, Geetha A, Thilagavathi M, Karvembu R, Krishnan V, Bertagnolli H, Natarajan K. (2004). Synthesis, characterization, EXAFS investigation and antibacterial activities of new ruthenium) III) complexes containing tetradentate Schiff base. J InorgBiochem. 98:2131–40.

[18] Uddin MN, Abdus Salam Md, Sultana J. (2015). Pb(II) complexes of Schiff bases derived from benzoylhydrazine as the antibacterial agents. Mod Chem. 3:7–14.

[19] Zhou X, Shao L, Jin Z, Liu J-B, Dai H, Fang J-X. (2007). Synthesis and antitumor activity evaluation of some Schiff bases derived from 2-aminothiazole derivatives. Heteroatom Chem. 18:55–9.

[20] Saadeh HA, AbuShaireh EA, Mosleh IM, Al-Bakri AG, Mubarak MS. (2012). Synthesis, characterization and biological activity of Schiff bases derived from metronidazole. Med Chem Res. 21: 2969-74.

[21] Parrey IR, Hashmi AA. (2015). Synthesis of Schiff base complexes ofMn(II) and Co(II) and their catalytic oxidation towards olefinsand alcohols. Can Chem Trans. 3:65–71.

[22] Balasubramanian KP, Karvembu R, Prabhakaran R, Chinnusamy V, Natarajan K. (2007). Synthesis, spectral, catalytic and antimicrobial studies of PPh3/AsPh3 complexes of Ru(II) with dibasic tridentate O, N, S donor ligands. SpectrochimActa, Part A. 68:50–4.

[23] Ali OAM. (2014). Palladium(II) and zinc(II) complexes of neutral [N2O2] donor Schiff bases derived from furfuraldehyde: synthesis, characterization, fluorescence and corrosion inhibitors of ligands.SpectrochimActa, Part A. 132:52–60.

[24] Bhkahk CK, Hadi JS. (2015). New unsymmetrical Schiff base as inhibitor of carbon steel corrosion and antibacterial activity. Res J Chem Sci. 5:64–70.

[25] Fouda AS, Ibrahim AA,El-behairy WT. (2014). Thiophene derivatives as corrosion inhibitors for carbon steel in hydrochloric acid solutions Der PharmaChemica, 6(5):144-157.

[26] ASTM, Standard Practice for Laboratory Immersion Corrosion Testing of Metals, G 31–72, ASTM, Philadelphia, PA (1990) 401.

[27] Salman Y, Barlas FB, Yavuz M, Kaya K, Timur S,Telli FÇ, (2018). Synthesis, characterization and biological application of dinuclearCu(II(complexes of Schiff base ligands of galactochloralose and α-chloralose.InorgChimActa.483:98–105.

[28] Mounika K, Anupama B, Pragathi J, Gyanakumari C. (2010). Synthesis¸ Characterization and Biological Activity of a Schiff Base Derivedfrom 3-Ethoxy Salicylaldehyde and 2-Amino Benzoic acid and its TransitionMetal Complexes. J. Sci. Res. 2:513-24.

[29] Byun JC, Mun DH, Park KM, (2014). Synthesis and Characterization of Compartmental Macrocyclic Binuclear Copper(II) Complex with BidentatePerchlorato Ligand. Bull. Korean Chem. Soc. 35:269-72.

[30] Nakamoto K. (1986). Infrared and Raman Spectra of Inorganic and Coordination Compounds, Wiley, New York, pp 227, 256 -257.

[31] Taha ZA, Ajlouni AM, Al Momani W. (2012). Structural, luminescence and biological studies of trivalent lanthanide complexes with N,N′-bis(2-hydroxynaphthylmethylidene)-1,3-propanediamine Schiff base ligand Journal of Luminescence 132:2832-41.

[32] Calu L, Badea M, Korošin NČ, Chifiriuc MC, Bleotu C, Stanică N, Silvestro L, Maurer M, Olar R.(2018). Spectral, thermal and biological characterization of complexeswith a Schiff basebearing triazole moiety as potential antimicrobialspecies. J. Therm. Anal. Calorim.134:1839-50.

[33] AranhaPE, dos Santos MP, RomeraS,Dockal ER. (2007). "Synthesis, characterization, and spectroscopic studies of tetradentate Schiff base chromium(III) complexes," Polyhedron.26:1373–82.

[34] Abd El-Wahab ZH, Mashaly MM, Salman AA, El-ShetaryBA,Faheim AA. (2004).Co(II), Ce(III) and UO2(VI) Bis-Salicylatothiosemicarbazide Complexes: Binary and Ternary Complexes, Thermal Studies and Antimicrobial Activity. SpectrochimActa, Part A. 60:2861–73.

[35] Abu-Hussen AAA, Linert W.(2009).Redox, thermodynamic and spectroscopic of some transition metal complexes containing heterocyclic Schiff base ligands.SpectrochimActa, Part A. 74:214-23.

[36] Mohamed GG, Omar MM, Hindy AMM. (2005). Synthesis, characterization and biological activity of some transition metals with Schiff base derived from 2-thiophene carboxaldehyde and aminobenzoic acid.SpectrochimActa, Part A. 62:1140-50.

[37] Zayed MA, Nour El-Dien FA, Mohamed GG, El-Gamel NEA. (2004). Structure investigation, spectral, thermal, X-ray and mass characterization of piroxicam and its metal complexes. SpectrochimActa, Part A. 60:2843-52.

[38] Mohamed GG, Abd El-Wahab ZH (2005). Mixed ligand complexes of bis(phenylimine) Schiff base ligands incorporating pyridinium moiety Synthesis, characterization and antibacterial activity. Spectrochim Acta, Part A. 61:1059-68.

[39] Ali OAM (2014). Synthesis, spectroscopic, fluorescence properties and biological evaluation of novel Pd (II) and Cd (II) complexes of NOON tetradentate Schiff bases.SpectrochimActa, Part A. 21:188-95.

[40] Refat MS, El-Metwaly NM. (2011). Spectroscopic and fluorescence studies on Mn(II), Co(II), Ni(II) and Cu(II) complexes with NO donor fluorescence dyes. SpectrochimActa, Part A. 81:215–27.

[41] Massoud AA, Hefnawy A, Langer V, Khatab MA, Öhrstrom L,Abu-Youssef MAM. (2009).Synthesis, X-ray structure and anti-corrosion activity of two new silver(I) pyrazino complexes. Polyhedron 28:2794–2802.

[42] Dharmaraj N, Viswanathamurthi P, Nataragan K (2001).Ruthenium(II) complexes containing bidentate Schiff bases and their antifungal activity.

[43] J. Transition Met. Chem. 26:105–09.

Citation: *Omyma Ahmed Moustafa Ali, et.al, "Spectroscopic, Thermal, Fluorescence Studies and Antibacterial Activity of Some Transition Metals with Schiff Base 2-[(2-Furylmethylene) Amino] Benzoic Acid", International Journal of Advanced Research in Chemical Science, vol. 6, no. 10, p. 7-21, 2019. DOI: http://dx.doi.org/10.20431/2349-0403.0610002*